

Energy absorption by metal-vapor-dominated plasma during carbon dioxide laser welding of steels

R. Miller and T. DebRoy

Department of Materials Science and Engineering, The Pennsylvania State University, University Park, Pennsylvania 16802

(Received 20 November 1989; accepted for publication 10 May 1990)

During laser welding, the plasma plume affects the amount of energy reaching the weld surface and the composition and properties of the welds. Light emissions during welding were recorded by emission spectroscopy to understand the energy absorption and the nature of the plasma formed during welding of various grades of steels. The flow of gases and the concentrations of the various metal vapors were computed by solving the Navier Stokes equation and the equations of conservation of various species. The variables studied were shielding gas composition and flow rate and the base metal composition. Until now, self-absorption of emissions arising from species present at high concentrations within the plasma has kept researchers limited to either analyzing ideal situations that are unrelated to the welding process or not accounting for the attenuation of the emissions. It is demonstrated that during welding, the peaks in the emission spectra that are affected by the self-absorption process can be eliminated on the basis of the initial and the terminal energy levels for electronic transitions. By selectively eliminating the affected transitions and by using the numerically computed local concentrations of metal vapors, the absorption of the laser beam energy by the plasma can be accurately determined.

I. INTRODUCTION

During laser welding, the transmission of the laser beam through the plasma plume that forms near the material surface is affected by the nature of the plasma. In most cases, the attenuation of the laser beam energy occurs mainly due to its interactions with the free electrons in the plasma and the extent of absorption depends on the electron density and the kinetic energy of the electrons, measured by the electron temperature. The procedure for the calculation of electron density in the welding plasmas is well documented in the literature. However, the procedure requires knowledge of the electron temperature in the plasma. In the classical approach to determine the electron temperature, light emissions at various wavelengths from the plasma¹⁻⁴ are analyzed by emission spectroscopy. One of the important features of the laser-induced plasmas is the high population density of the various metal vapor species at various levels of excitation. Because of the high concentration of the various species, a portion of the photons that are emitted from within the plasma domain can be reabsorbed by other species at the emissions terminating state, and remains undetected, thus lowering the measurable emission intensity. As a result, the recorded intensity at certain wavelengths becomes lower than the true intensity of emission. Until now, this phenomenon of self-absorption of emissions arising from species present at high concentrations within the plasma, in most cases, has kept researchers limited to either analyzing ideal systems using low species concentration which is unrealistic for welding systems or, even worse, not accounting for the self-absorption effect at all and thus often incurring unacceptably large errors. In this paper, a method⁵ is demonstrated to assess self-absorption and selectively eliminate affected emissions from analyses, resulting in accurate treatment of the data.

The concentrations of the various metallic constituents of the plasma depend on the vaporization rates of the various alloying elements. In order to determine the true extent of absorption of the CO₂ laser radiation by the plasma plume, both experimental and theoretical calculations are utilized in this work. The light emissions from the plasma are monitored to determine the species present in the plasma and the electron temperature associated with the plasma for various alloys and welding conditions. The experimental data on the rates of vaporization of various metal vapors are coupled with computed fluid flow fields in the gas phase to predict the concentration profiles of the various species. Electron densities are computed from these profiles at various locations in the plasma domain and the total laser beam energy absorption due to the free electrons is then determined for various conditions. The shielding gas composition and flow rate, and the base metal composition are among the major parameters assessed in trying to arrive at the optimal low absorption conditions required to produce high-energy efficient weldments.

II. EXPERIMENTAL DETAILS

A Coherent Everlase model 525-1 carbon dioxide laser was used in the enhanced pulse mode to weld AISI 201 stainless steel, 99.999% pure iron, and a variety of plain carbon steels ranging in carbon content from 0.1% to 0.8%. The pulse mode laser was operated at a frequency of 100 Hz and a pulse length of 0.003 s, yielding a 30% duty cycle at a tube current of 50 mA. The laser beam was focused perpendicularly on to the surface of the target by a 0.13-m focal length, antireflection-coated Zn-Se lens. The focused beam had a spot size of approximately 0.000 28 m which resulted in a power density of about 4×10^{10} W/m² throughout the experiments. The targets were mounted onto a computer-con-

trolled translation table which moved at a rate of 0.005 m/s.

Emissions from the plasma were monitored using a Princeton Applied Research Corporation model 1254 M1216 Silicon Intensified Target detector coupled with a model 1460-V optical multichannel analyzer system. The emissions were focused onto the slit of the monochromator, which was parallel to the axis of the laser beam, by a convex lens as shown in Fig. 1. A 2400 grooves/mm diffraction grating was employed for increased peak resolution.

The shielding gas, 99.999% pure argon, was passed coaxially with the laser beam through a 0.00175-m-radius copper nozzle at a height of 0.018 m above the target surface. The shielding gas velocity and composition was varied, however, when checking the effects of the parameters on the plasma.

To keep all samples uniform for analysis, since surface roughness affects laser absorption by the target workpiece, samples were polished with 240 grit paper until they were level and smooth. The samples were then cleaned with acetone to remove any dirt or loose particles which would also affect laser absorption.

III. RESULTS AND DISCUSSION

Upon identification of the lines in the spectra obtained during welding of stainless steel, shown in Fig. 2, it can be observed that only iron, manganese, and chromium emissions are detected. Although nickel and other base metal elements as well as argon shielding gas atoms are present, no emissions are detected due to low vapor pressures of the metallic elements and the high ionization potential of argon. Previous investigators who have not found shielding gas emissions in the spectra have reported low temperatures, while investigators obtaining argon peaks report temperatures as high² as 17 000 K. The electron temperature within the plasma can be determined from the intensities of emissions at various wavelengths for a particular element. The procedure is given in Boumans⁶ and only a brief summary is presented here. Combination of the equation for absolute intensity of an atom line with an expression for the Boltzmann distribution of energy-level populations yields an expression of the following form:

$$\ln(I/gA\nu) = \ln C - (E_q/kT), \quad (1)$$

where I is the integrated intensity in s^{-2} , g is the degeneracy

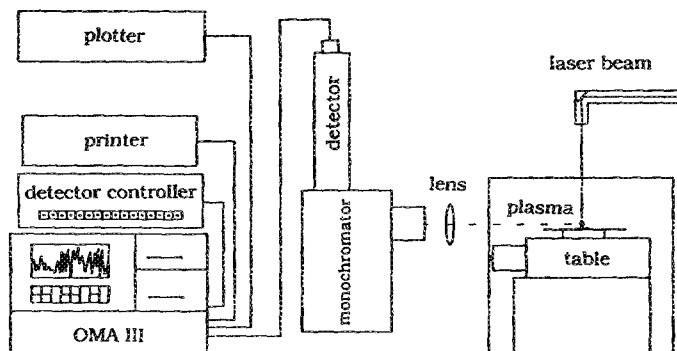


FIG. 1. Schematic representation of the experimental setup.

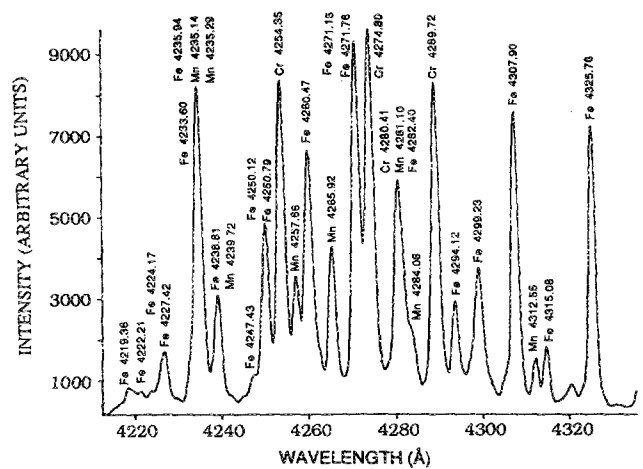


FIG. 2. Typical spectra recorded for pulsed laser welding of AISI 201 stainless steel. Pulse length = 0.003 s, frequency = 100 Hz, argon flow rate = 50 ml/s, current = 50 mA, and welding speed = 0.005 m/s.

of the upper-energy level q , A is the transition probability for the transition from state q to the lower-energy level in s^{-1} , ν is the frequency in s^{-1} , E_q is the energy associated with the level q in cm^{-1} , k is the Boltzmann constant in $cm^{-1} K^{-1}$, T is the electron temperature in K, and C is a constant.

The electron temperature can be obtained from the slope of the plot showing the left-hand-side term in Eq. (1) versus E_q . Figure 3 shows a Boltzmann plot obtained from the regression of 13 excited neutral iron emissions during welding of 1035 steel. Values of g , A , and E_q were taken from Fuhr⁷ for the iron peaks. From the slope of the plot, an apparent electron temperature of over 14 000 K is obtained. However, it will be demonstrated that the result is not accurate since all the peak intensities were used to obtain the temperature without correction for self-absorption.

Using a formalism suggested by Peebles,⁵ which utilizes the ratio of two peak intensities originating from the same upper-energy state, the extent of self-absorption was assessed. Consider two emission lines, A and B , whose intensity equations⁶ are, respectively,

$$I_A = (dh/4\pi)A_A n_A \nu_A, \quad (2)$$

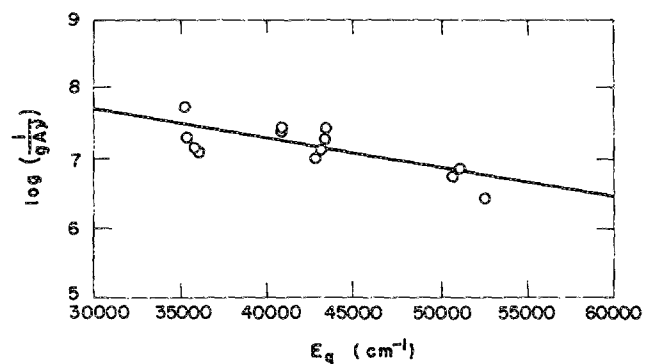


FIG. 3. Boltzmann plot used to determine the average electron temperature of the plasma formed during pulsed laser welding of AISI 1035 steel. No correction was made for the self-absorption. Pulse length = 0.003 s, frequency = 100 Hz, argon flow rate = 50 ml/s, current = 50 mA, and welding speed = 0.005 m/s.

$$I_B = (dh/4\pi)A_B n_B \nu_B, \quad (3)$$

where I is the absolute intensity in $\text{erg cm}^{-2} \text{s}^{-1}$, d is the depth in cm, h is the Planck's constant in erg s, A is the transition probability in s^{-1} , n is the density of the species present at the excited state being considered in cm^{-3} , and ν is the frequency of the emitted photon in s^{-1} . If both transitions start from the same excited state in the same source, then $n_A = n_B$, and thus the ratio of the two intensities is given by the following equation in the absence of self-absorption:

$$I_A/I_B = A_A \nu_A / A_B \nu_B. \quad (4)$$

The computed values of I_A/I_B can be compared with the experimental data for agreement. If self-absorption is present, the expression becomes more complicated and in the case of extremely high self-absorption, the ratio of the two peak intensities approaches unity, rather than the value obtained by Eq. (4). Table I shows the comparison of the theoretical and the experimental ratios for the six pairs of peaks. It is observed that the transitions terminating near $12\,000 \text{ cm}^{-1}$ are subjected to strong self-absorption, while those terminating above $17\,000 \text{ cm}^{-1}$ agree fairly well between experimental and theoretical values, implying that self-absorption is not a very serious problem above $17\,000 \text{ cm}^{-1}$, where species densities are not great enough to produce significant self-absorption effects. Utilizing this information, the data in Fig. 2 were replotted using only the peaks corresponding to transitions which terminate above $17\,000 \text{ cm}^{-1}$. A temperature of about 8630 K was calculated from this plot and a confidence level of $\pm 400 \text{ K}$ was estimated from the error analysis with a 90% confidence level. The difference between the values of the electron temperatures obtained with and without the self-absorption correction demonstrates the importance of the selection of peaks for the Boltzmann plots. Failure to take appropriate precautions in the temperature calculations can lead to large errors in the

TABLE I. Comparison of the theoretical and experimental ratios for the product of the frequency and the transition probability for various peak pairs whose transitions begin at the same upper-energy state.

Peaks (Å)	Theory	Actual	Upper (cm^{-1})	Terminate (cm^{-1})
$\frac{\lambda_A}{\lambda_B}$	$\frac{A_A \nu_A}{A_B \nu_B}$	$\frac{I_A}{I_B}$	E_q	$\frac{E_{Ap}}{E_{Bp}}$
$\frac{4307}{4202}$	4.154	0.816	35 768	$\frac{11\,976}{12\,561}$
$\frac{4063}{4132}$	5.398	1.736	37 163	$\frac{12\,561}{12\,969}$
$\frac{4071}{4005}$	3.577	1.760	37 521	$\frac{12\,561}{12\,969}$
$\frac{4282}{4315}$	1.232	1.291	40 895	$\frac{17\,550}{17\,727}$
$\frac{4260}{4235}$	1.599	1.532	42 816	$\frac{19\,351}{19\,562}$
$\frac{4238}{4247}$	1.102	1.057	50 980	$\frac{27\,395}{27\,167}$

TABLE II. Temperatures calculated for laser welding of AISI 201 stainless steel while varying argon flow rate from 1 to 8 //min and the average electron temperatures for the welding of various grades of carbon steels based on eight runs for each type of steel.

Ar flow rate (LPM)	Temperature (K)	Type of steel	Average T_e (K)
1.0	8707	1010	8775 ± 400
1.5	9251	1035	8634 ± 400
2.0	8766	1040	8818 ± 400
2.5	9212	1080	8713 ± 400
3.0	8675		
4.0	9193		
5.0	9116		
6.0	8907		
7.0	8768		
7.5	8835		
8.0	8737		

electron temperature and in the estimation of the amount of laser beam energy absorption by the plasma.

Table II summarizes the effect on the average electron temperature from varying the shielding gas flow rate and the carbon content of the base metal. In both cases, no effect was noticed, with the average temperature being about 8800 K . Although increasing the flow rate of the argon shielding gas did not affect the average electron temperature, it did dramatically reduce the size of the plasma domain by convectively transporting away the components of the plasma. Figure 4 shows direct evidence of this. Since the intensity of an

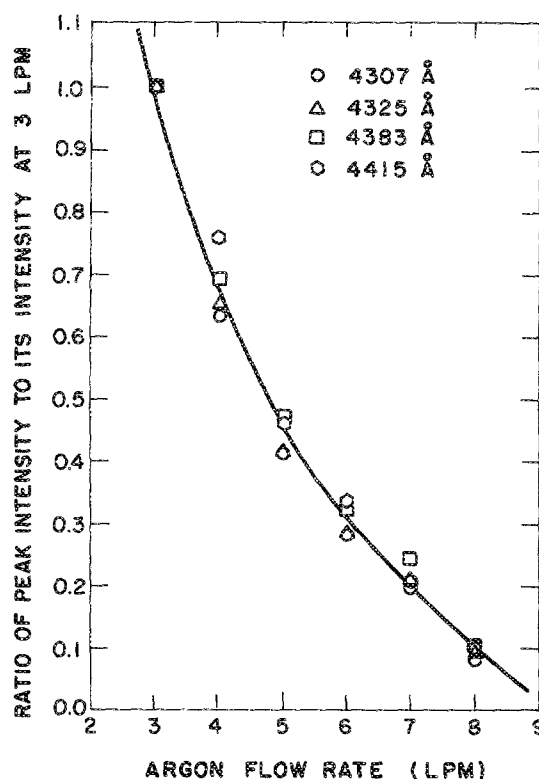


FIG. 4. Ratios of the intensities of various emissions at a given flow rate of Ar to the emission's intensities at a flow rate of 50 ml/s (3 //min) as a function of Ar shielding gas flow rate.

emission line is proportional to the depth of the source volume, and the intensities decrease dramatically as the flow rate is increased, the plasma plume must grow smaller with the increased flow, all the other parameters remaining constant. Experiments with helium shielding gas demonstrated a similar behavior. Although the plasma volume and the spectral intensities were considerably smaller while welding with helium, or a mixture of argon or helium, the electron temperatures were essentially constant at a value of 8800 ± 400 K. It is interesting to note that Key, Chan, and McIlwain⁸ also found that the shielding gas composition has a significant effect on plasma volume and radial temperature distribution but not on the peak temperature in the interior of the plasma during GTA welding. The spectra for the various carbon steels did not show a noticeable difference among themselves and the rates of vaporization of the various species did not change appreciably. Variation of the carbon content within the concentration range investigated did not significantly change the plasma properties.

The two most important parameters necessary to assess the absorption are the temperature and the electron density. To determine the electron density, the approach of Dunn and Eagar⁹ was employed. In this approach, the total electron density, n_e , is assumed to be the summation of the mole fractions of each species present in the plasma, x_i , multiplied by the electron density in a plasma comprised solely of each species at the given temperature, n_i' , as follows:

$$n_e = \sum_{i=1}^n x_i n_i' \quad (5)$$

The quantity n_i' is found from Fig. 5 which shows the computed results of the electron density through solution of Saha's equation for equilibrium between an electron and an atom as was done by Dunn and Eagar.⁹ They present an

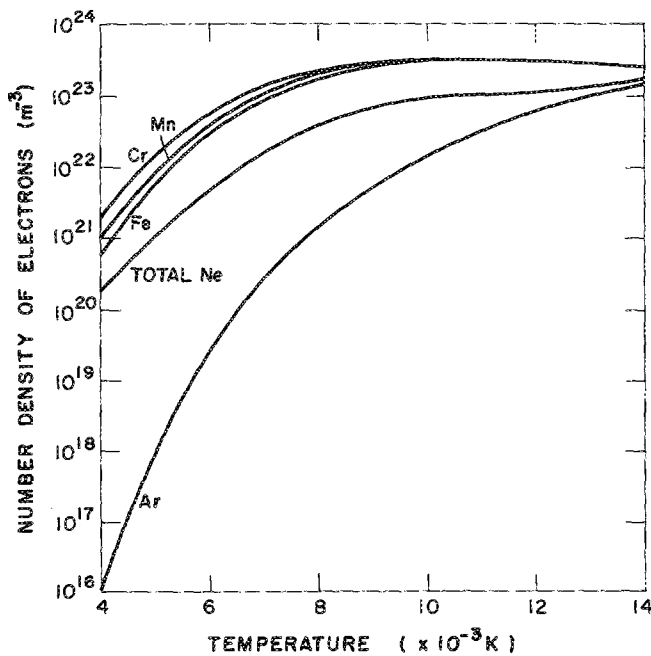


FIG. 5. Electron density as a function of temperature for various species in a pure plasma comprised solely of that single species. After the work of Dunn and Eagar (see Ref. 9).

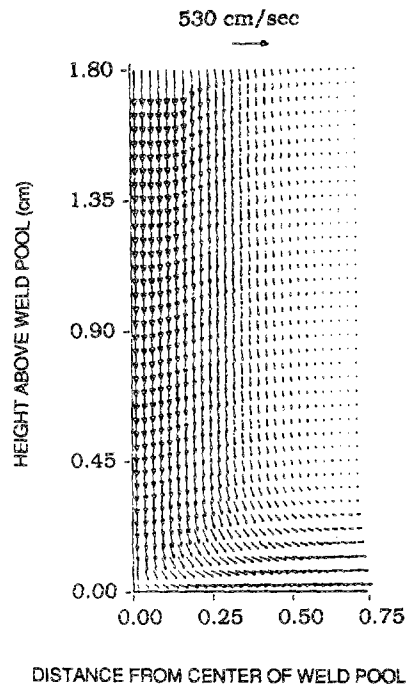


FIG. 6. Velocity profile for the argon shielding gas.

excellent explanation of the computational process and this is not discussed here. The mole fraction, however, must be computed for various regions of the plasma from the concentration profiles of the various species present in the plasma.

To calculate the concentration profile, the flow field of the shielding gas must be known, as it is responsible for all the convective transport of heat and mass. Figure 6 shows

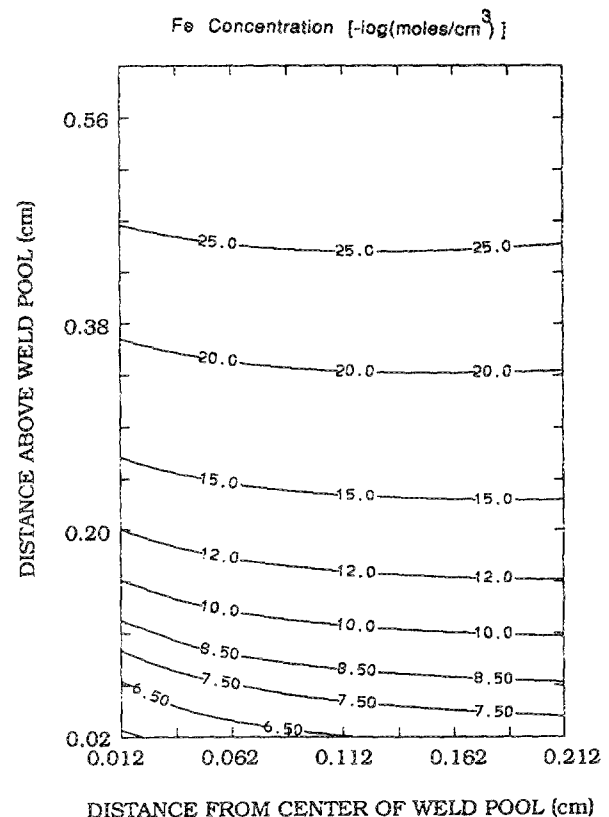


FIG. 7. Concentration profiles of iron vapor near the weld pool.

TABLE III. Summary of absorption calculations as a function of height during pulsed laser welding of AISI 201 stainless steel using 600 W incident power and 50 ml/s argon flow rate, incident beam is perpendicular to the sample, and the electron temperature is 8800 K. % absorption = 29.71%.

Height (cm)	Ne total (No./cm ³)	K_e (cm ⁻¹)	Intensity (W)
0.16	4.16×10^{15}	0.003	599.98
0.15	4.18×10^{15}	0.003	599.96
0.14	4.18×10^{15}	0.003	599.95
0.13	4.20×10^{15}	0.003	599.93
0.12	4.22×10^{15}	0.003	599.91
0.11	4.29×10^{15}	0.003	599.89
0.10	4.44×10^{15}	0.004	599.87
0.09	4.81×10^{15}	0.005	599.85
0.08	5.13×10^{15}	0.010	599.82
0.07	7.50×10^{15}	0.026	599.76
0.06	1.23×10^{16}	0.114	599.60
0.05	2.56×10^{16}	0.630	598.92
0.04	6.02×10^{16}	2.783	595.16
0.03	1.27×10^{17}	9.094	578.82
0.02	2.29×10^{17}	11.285	528.51
0.01	2.55×10^{17}	11.285	472.11
0.00	2.55×10^{17}		421.72

the velocity distribution for the argon shielding gas exiting the 0.001 75-m-radius nozzle at a rate of 50 ml/s at a height of 0.018 m above the target. The profile was computed by solving the appropriate Navier Stokes equation and the details of the calculations are available elsewhere.^{10,11} The flow is strong in the downward direction along the laser axis near the gas nozzle, but then reaches a stagnation point at the specimen surface. The vectors indicate that any heat or vapors exiting the weld pool should be carried radially away from the center by convection. However, the metal vapors can be transported upward by diffusion.

Knowledge of the flow field and temperature distribution, coupled with the data on vaporization rates and diffusivities of the metal vapors, can be used to calculate the necessary concentration profiles. Figure 7 shows the concentration profiles of iron vapors above the weld pool. The contours tend to slope upward as they approach the laser beam axis. Near the weld pool the shielding gas jet tends to stagnate, allowing the vapors to diffuse upward. In this region, high concentrations of metal vapors and electron densities are obtained. Thus, the region capable of largest absorption lies along the beam axis, just above the surface of the weld. The mole fraction of each species can be determined for the various plasma regions from the concentration profiles of various species, and hence the total electron density can be calculated throughout the plasma domain from Eq. (5).

The inverse bremsstrahlung absorption coefficient, k_e , can be determined for each volume element of the plasma by the following expression:

$$k_e = 1.62 \times 10^{-34} (n_e^t)^2 / \sqrt{T}, \quad (6)$$

where the constant 1.62×10^{-34} is valid for 10.6 μm radiation. The intensity of the laser beam exiting each cell can then be found using the exponential absorption law:

$$I = I_0 e^{-k_e \Delta y}, \quad (7)$$

where I_0 is the intensity entering the cell and Δy is the distance through the cell.

Table III summarizes the absorption calculations for the general case found in this work, consisting of the electron temperature of 8800 K, an argon flow rate of 50 ml/s, and appropriate vaporization rates of the various elements produced by the laser welding process.¹² If a 600-W incident laser beam entered the plasma plume, about 30% of the incident radiation would be absorbed by the plasma before it reached the target. Electron densities less than about $10^{22}/\text{m}^3$ do not account for very much absorption via the inverse bremsstrahlung process and almost all of the absorption occurs just above the weld pool.

Similar absorption calculations were performed for other gas flow rates and the results are shown in Fig. 8. Dilution of the metal vapors by the inert shielding gas is responsible for decreasing the mole fraction of metal vapors as the shielding gas flow rate is increased. Experimental findings presented in Fig. 4 showing that the plasma volume decreases with the increase in the gas flow rate is consistent with these calculations. The decrease in the mole fraction becomes less pronounced as flow rate is increased and the absorption follows the same manner, but not proportionally. This is because the amount of absorption drops off more slowly than the mole fraction of the metal vapors due to the exponential absorption law, i.e., Eq. (7). Between 1 and 8

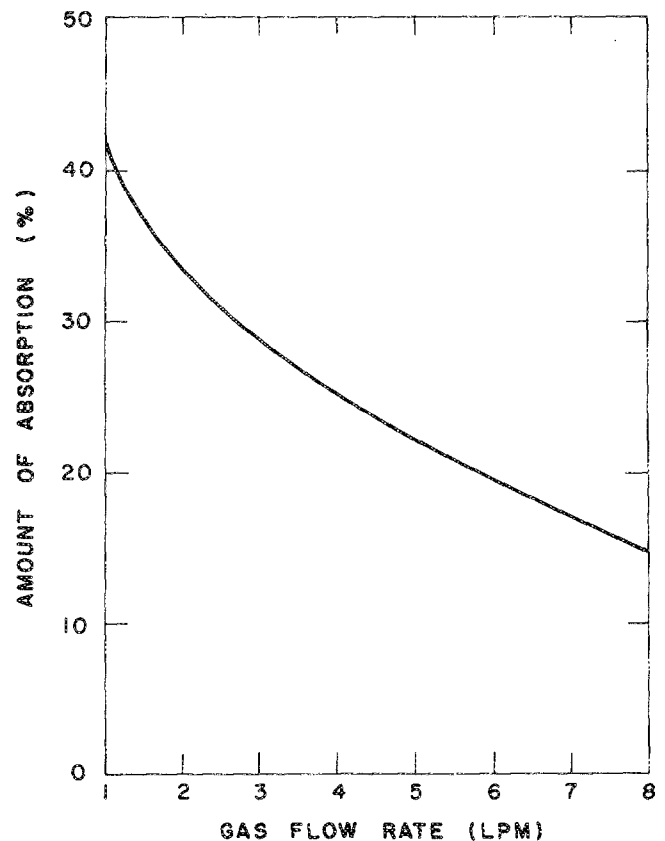


FIG. 8. Variation of the amount of absorption of the incident beam with argon shielding gas flow rate.

€/min, the absorption varies from about 42% to 15%, with most of the decrease occurring at low flow rates. The calculated absorption values are consistent with the range of values reported in the literature during laser welding with as high as 80% for high-power laser welding² and as low as 15% for low-power welding¹⁰ being absorbed. Calculations demonstrate that if all the variables remain constant, the absorption varies dramatically as the electron temperature changes, varying from virtually none at temperatures less than 5000 K to about 52% at 14 000 K using argon as the shielding gas. The relationship between the absorption and the electron temperature is dictated primarily by the properties of the shielding gas involved. The large variation in the amount of absorption with electron temperature demonstrates how crucial it is to accurately assess the temperature. For example, not accounting for the self-absorption effect at high species concentrations can invalidate laser absorption calculations.

IV. CONCLUSIONS

During laser welding of steels, a significant proportion of the incident radiation never reaches the target surface due to absorption of the beam energy by the plasma plume. Although strong evidence is shown for self-absorption of light emissions during laser welding of steels, it is demonstrated that a species present in high concentrations in the plasma such as iron can still be utilized as a thermometric element for the determination of the electron temperature. Peaks affected by self-absorption can be identified by comparing the experimental and theoretical intensity ratios for transitions starting from the same upper energy state, and avoided in the

analysis. For the welding of AISI 201 stainless steel, the species identified are excited neutral atoms of iron, manganese, and chromium. No other elements, including the shielding gas elements, were detected in the wavelength range investigated. Changes in the shielding gas flow rate or composition did not affect the electron temperature. However, increasing the flow rate of the shielding gas reduced the volume of the plasma plume. No variations in either the size or the electron temperature of the plasma were observed for the welding of various grades of carbon steels.

ACKNOWLEDGMENTS

Appreciation is expressed to Dr. H. C. Peebles of the Sandia National Laboratories for helpful discussions and communications. The work was supported by the U.S. Department of Energy, Office of Basic Energy Sciences, Division of Materials Science, under Grant No. DE-FGO2-84ER45158.

- ¹J. Knudtson, W. Green, and D. Sutton, *J. Appl. Phys.* **61**, 4771 (1987).
- ²T. Rockstroh and J. Mazumder, *J. Appl. Phys.* **61**, 917 (1987).
- ³M. M. Collur and T. DebRoy, *Metall. Trans. B* **20**, 277 (1989).
- ⁴J. C. Chennat and C. E. Albright, *Proceedings of the ICALEO, Laser Institute of America*, Vol. 44, pp. 76-85 (1984).
- ⁵H. C. Peebles (private communication).
- ⁶P. W. J. M. Boumans, *Theory of Spectrochemical Excitation* (Hilger and Watts, London, 1966).
- ⁷J. T. Fuhr (private communication).
- ⁸J. F. Key, J. W. Chan, and M. E. McIlwain, *Welding J.* **62**, 179 (1983).
- ⁹G. J. Dunn and T. W. Eagar, *Metall. Trans. A* **17**, 1865 (1986).
- ¹⁰M. M. Collur, Ph.D. thesis, Pennsylvania State University, 1988.
- ¹¹R. Miller, M.S. thesis, Pennsylvania State University, 1989.
- ¹²P. A. A. Khan, Ph.D. thesis, Pennsylvania State University, 1987.